

SELF-SIMILARITY OF PION PRODUCTION IN AA COLLISIONS AT RHIC¹

M. V. Tokarev^{a,2}, *I. Zborovský*^{b,3}

^a Joint Institute for Nuclear Research, Dubna

^b Nuclear Physics Institute, Academy of Sciences of the Czech Republic,
Řež, Czech Republic

Experimental data on inclusive spectra of pions produced in heavy-ion collisions at RHIC are analyzed in the framework of z -scaling. The data indicate similarity as a characteristic feature of the mechanism of pion production at high energies. It is argued that this property includes structure of the colliding objects, interaction of their constituents, and character of the fragmentation process. A microscopic scenario of nucleus interactions at a constituent level in terms of momentum fractions is developed. The centrality dependence of the shape of the scaling function $\psi(z)$ and the fractal dimension ϵ_{AA} of the fragmentation process is studied. Energy losses of particles in the final state as a function of the collision energy, transverse momentum, and centrality are estimated. The scale dependence of the energy losses is discussed. A decreasing tendency of specific heat of the produced medium with the system size is established. The obtained results may be exploited to search for and study new physics phenomena in pion production in pp and AA collisions at high multiplicities.

Проведен анализ экспериментальных данных по инклюзивным сечениям рождения пионов в релятивистских столкновениях тяжелых ионов на RHIC в рамках z -скейлинга. Показано, что свойство самоподобия является характерной особенностью рождения пионов при столкновениях ядер высоких энергий. Обосновывается его связь со структурой сталкивающихся ядер, взаимодействием их конститuentов и механизмами процесса фрагментации. Предложен микроскопический сценарий взаимодействия ядер на уровне конститuentов. Исследована зависимость формы функции $\psi(z)$ и фрактальной размерности ϵ_{AA} от центральности столкновения. Получены оценки потерь энергии пионов в среде в зависимости от его поперечного импульса, энергии и центральности столкновения ядер. Обсуждается зависимость величины потерь от масштаба, на котором происходит взаимодействие конститuentов. Установлено уменьшение «удельной теплоемкости» ядерной среды с ростом атомного номера ядра. Полученные результаты могут быть использованы для поиска и изучения новых явлений в процессах с рождением пионов в pp - и AA -столкновениях высоких энергий и при больших множественностях.

PACS: 25.75.Bh; 24.80.+y; 11.30.Ly

¹Talk presented at the Conference Session of RAS Physics Sciences Department, «Physics of Fundamental Interactions», ИФЕР, Protvino, December 22–25, 2008.

²E-mail: tokarev@sunhe.jinr.ru

³E-mail: zborovsky@ujf.cas.cz

INTRODUCTION

The measurements of particle spectra at the Relativistic Heavy Ion Collider (RHIC) led to the discovery of a substantial suppression of hadron yields in nucleus–nucleus collisions relative to proton–proton data [1–4]. The suppression is observed in the region of high transverse momenta, typically more than a few GeV/ c . It is connected with the energy radiations of the outgoing high- p_T partons propagating through dense matter formed in the central collisions of heavy nuclei. The energy losses in the dense medium are substantially larger than in the vacuum. Quantification of the effect in the final state is a difficult problem depending on complicated calculations and model assumptions.

In the paper we analyze spectra of pions produced in heavy-ion collisions at RHIC and develop a microscopic scenario of the spectra suppression in the framework of data z -presentation. The approach was applied for analysis of hadron production in pp and $\bar{p}p$ collisions at high energies [5]. The above systems represent collisions of extended objects interacting in terms of their constituents. Production of particles from the constituent interactions is governed by the principles of self-similarity, locality, and fractality. The self-similarity of hadron production is valid in both soft and hard physics [6]. The locality and fractality are applied to the hard processes at small scales. The principles are manifested by the z -scaling observed in the production of charged and identified hadrons in pp and $\bar{p}p$ collisions. The scaling represents independence of the scaling function $\psi(z)$ from the collision energy, types of the inclusive hadrons, and their production angles, and includes spectra for various selection criteria with different charged multiplicities N_{ch} [7]. The general principles can be applied to the nucleus–nucleus interactions as well. Here we demonstrate that pion spectra for different centrality classes in AA collisions characterized by different multiplicity densities $dN_{\text{ch}}/d\eta$ exhibit similar scaling behavior as in pp collisions. This holds in a wide range of the transverse momentum p_T and the collision energy \sqrt{s} . The shape of the function $\psi(z)$ for AA systems depends on the collision centrality and differs from the scaling function for pp interactions at high z . In the considered case of pions, a linear dependence of the fractal dimension ϵ_{AA} of the fragmentation process on the multiplicity density $dN_{\text{ch}}/d\eta$ allows us to restore the centrality independent shape of $\psi(z)$ for AA collisions which is identical with the z -scaling in pp interactions. The increase of ϵ_{AA} with the multiplicity density is connected with larger energy losses of high- p_T particles in the collisions of heavy nuclei. The region of small p_T is characterized by low values of the scaling variable z . The single parameter c which controls the behavior of $\psi(z)$ at low z is interpreted as a «specific heat» of the produced medium. Performed analysis shows that it is independent of collision centrality but depends on the type of the colliding nuclei. Search for a possible change in the parameter c is of interest especially for soft processes with high multiplicities. Such a change could be an indication of a phase transition in the matter produced in high energy collisions of both hadrons and nuclei.

The paper is organized as follows. A concept of the z -scaling and the method of construction of the scaling function $\psi(z)$ for both hadron and nucleus collisions are briefly described in Sec. 1. The properties of $\psi(z)$ for pion production in pp collisions are mentioned in Sec. 2. Results of analysis of pion spectra measured in AA collisions at RHIC and SpS are presented in Sec. 3. Pion production in dAu collisions is studied in Sec. 4. A microscopic scenario of the elementary subprocesses in AA collisions is discussed and energy losses of the secondary particles are estimated in Sec. 5. Conclusions are summarized in the final section.

1. INCLUSIVE SPECTRA IN z -PRESENTATION

In this paper we follow the version of the z -scaling presented in [5, 6]. Let us briefly remind the basic ideas of this concept. It is assumed that the collision of extended objects like hadrons and nuclei at sufficiently high energies is considered as an ensemble of individual interactions of their constituents. The constituents are partons in the parton model or quarks and gluons in the theory of QCD. A single interaction of constituents is illustrated in Fig. 1.

Structures of the colliding objects are characterized by parameters δ_1 and δ_2 . The constituents of the incoming objects (hadrons or nuclei) with masses M_1, M_2 and momenta P_1, P_2 carry their fractions x_1, x_2 . The inclusive particle carries the momentum fraction y_a of the scattered constituent with a fragmentation characterized by a parameter ϵ_a . A fragmentation of the recoil constituent is described by the parameter ϵ_b and the momentum fraction y_b . Multiple interactions of constituents are considered to be similar. This property reflects a self-similarity of the hadronic interactions at the constituent level.

1.1. Momentum Fractions x_1, x_2, y_a , and y_b . The idea of the z -scaling is based on the assumption [8] that gross features of an inclusive particle distribution of the reaction

$$M_1 + M_2 \rightarrow m_1 + X \quad (1)$$

can be described at high energies in terms of the kinematical characteristics of the corresponding constituent subprocess. We consider the subprocess to be a binary collision

$$(x_1 M_1) + (x_2 M_2) \rightarrow \left(\frac{m_1}{y_a} \right) + \left(x_1 M_1 + x_2 M_2 + \frac{m_2}{y_b} \right) \quad (2)$$

of the constituents $(x_1 M_1)$ and $(x_2 M_2)$ resulting in the scattered (m_1/y_a) and recoil $(x_1 M_1 + x_2 M_2 + m_2/y_b)$ objects in the final state. The produced secondary objects transform into real particles after the constituent collisions. The registered particle with the mass m_1 and the 4-momentum p and its hadron counterpart, moving in the opposite direction, carry the momentum fractions y_a and y_b of the scattered and recoil systems, respectively. The momentum conservation law of the constituent subprocess is connected with a recoil mass M_X which we write in the form

$$\left(x_1 P_1 + x_2 P_2 - \frac{p}{y_a} \right)^2 = M_X^2, \quad (3)$$

where $M_X = x_1 M_1 + x_2 M_2 + m_2/y_b$. The associate production of (m_2) ensures conservation of the additive quantum numbers. Equation (3) is an expression of the locality of the hadron

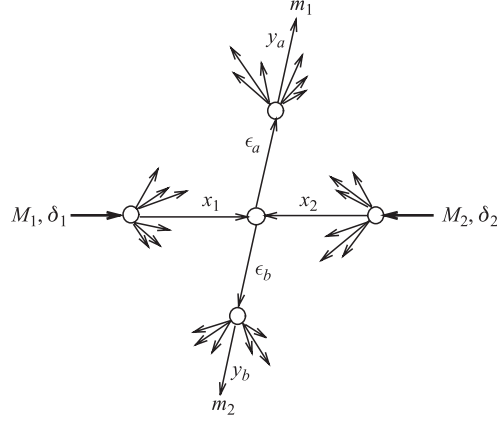


Fig. 1. Diagram of the constituent subprocess

interaction at a constituent level. It represents a kinematical constraint on the momentum fractions x_1 , x_2 , y_a , and y_b which determine a subprocess (2).

Structure of the colliding objects and fragmentation of the systems formed in the scattered and recoil directions are characterized by the parameters δ_1, δ_2 and ϵ_a, ϵ_b , respectively. We connect the structural parameters with the corresponding momentum fractions by the function

$$\Omega(x_1, x_2, y_a, y_b) = (1 - x_1)^{\delta_1} (1 - x_2)^{\delta_2} (1 - y_a)^{\epsilon_a} (1 - y_b)^{\epsilon_b}. \quad (4)$$

Physical interpretation of Ω is given by its proportionality to relative number of all such constituent configurations in the reaction (1) which contain the configuration defined by the fractions x_1, x_2, y_a , and y_b . The function Ω plays the role of a relative volume which is occupied by these configurations in the space of the momentum fractions. It was found that the structural parameters δ_1 and δ_2 have constant values at high energies. This holds for ϵ_a and ϵ_b in pp collisions as well. The parameters are interpreted as fractal dimensions in the corresponding space of the momentum fractions. For proton–proton collisions we set $\delta_1 = \delta_2 \equiv \delta$. In the case of nucleus–nucleus collisions there are relations $\delta_1 = A_1 \delta$ and $\delta_2 = A_2 \delta$, where A_1, A_2 are atomic numbers. We assume that the fragmentation of the objects moving in the scattered and recoil directions can be described by the same parameter $\epsilon_a = \epsilon_b \equiv \epsilon_F$ which depends on the type (F) of the inclusive particle. For given values of δ and ϵ_F , we determine the fractions x_1, x_2, y_a , and y_b in a way to maximize the function $\Omega(x_1, x_2, y_a, y_b)$, simultaneously fulfilling the condition (3). The momentum fractions x_1 and x_2 obtained in this way can be decomposed as follows:

$$x_1 = \lambda_1 + \chi_1, \quad x_2 = \lambda_2 + \chi_2, \quad (5)$$

where $\lambda_{1,2} = \lambda_{1,2}(y_a, y_b)$ and $\chi_{1,2} = \chi_{1,2}(y_a, y_b)$ are specific functions [5] of y_a and y_b . By using the decomposition, the subprocess (2) can be rewritten into a symbolic form

$$x_1 + x_2 \rightarrow (\lambda_1 + \lambda_2) + (\chi_1 + \chi_2). \quad (6)$$

This relation means that the λ -parts of the interacting constituents contribute to the production of the inclusive particle, while the χ -parts are responsible for the creation of its recoil.

Since the momentum fractions are determined by means of the maximization of expression (4), they implicitly depend on δ and ϵ_F . The parameter ϵ_F takes effectively into account also prompt resonances out of which the inclusive particle of a given type may be created. At fixed mass parameter m_2 , larger values of ϵ_F correspond to smaller y_a and y_b , which in turn give larger ratios m_2/y_b and m_1/y_a . In our phenomenological approach this means that production of the inclusive particle (m_1) and its counterpart (m_2) is a result of fragmentation from larger masses which mimic in a sense processes with prompt resonances. Values of these parameters are determined in accordance with self-similarity requirements and experiment. In particular, this gives the restriction $m_2 = m_1$.

1.2. Scaling Variable z and Scaling Function $\psi(z)$. The self-similarity of hadron interactions reflects a property that hadron constituents and their interactions are similar. This is connected with dropping of certain dimensional quantities out of the description of physical phenomena. The self-similar solutions are constructed in terms of the self-similarity parameters. We search for a solution

$$\psi(z) = \frac{1}{N\sigma_{\text{inel}}} \frac{d\sigma}{dz} \quad (7)$$

depending on a single self-similarity variable z . Here σ_{inel} is an inelastic cross section of the reaction (1) and N is an average particle multiplicity. The variable z is defined as follows:

$$z = z_0 \Omega^{-1}, \quad (8)$$

where

$$z_0 = \frac{\sqrt{s_{\perp}}}{(dN_{\text{ch}}/d\eta|_0)^c m} \quad (9)$$

and Ω given by (4). For a given reaction (1), z is proportional to the transverse kinetic energy $\sqrt{s_{\perp}}$ of the constituent subprocess (2) consumed on the production of the inclusive particle (m_1) and its counterpart (m_2). The energy $\sqrt{s_{\perp}}$ is determined by the formula

$$\sqrt{s_{\perp}} = T_a + T_b, \quad (10)$$

where

$$T_a = y_a(\sqrt{s_{\lambda}} - M_1\lambda_1 - M_2\lambda_2) - m_1, \quad T_b = y_b(\sqrt{s_{\chi}} - M_1\chi_1 - M_2\chi_2) - m_2. \quad (11)$$

The terms

$$\sqrt{s_{\lambda}} = [(\lambda_1 P_1 + \lambda_2 P_2)^2]^{1/2}, \quad \sqrt{s_{\chi}} = [(\chi_1 P_1 + \chi_2 P_2)^2]^{1/2} \quad (12)$$

represent the energy for production of the secondary objects moving in the scattered and recoil directions, respectively. The quantity $dN_{\text{ch}}/d\eta|_0$ is the corresponding multiplicity density of charged particles in the central region of the reaction (1) at pseudorapidity $\eta = 0$. The multiplicity density in the central interaction region is related to a state of the produced medium. The parameter c characterizes properties of this medium [5]. It is determined from multiplicity dependence of inclusive spectra [5–7]. The mass constant m is arbitrary and we fix it at the value of nucleon mass.

The scaling function $\psi(z)$ is expressed in terms of the experimentally measured inclusive cross section $E d^3\sigma/dp^3$, the multiplicity density $dN/d\eta$ at pseudorapidity η , and σ_{inel} . Exploiting the definition (7), one can obtain the expression [5]

$$\psi(z) = -\frac{\pi s}{(dN/d\eta)\sigma_{\text{inel}}} J^{-1} E \frac{d^3\sigma}{dp^3}, \quad (13)$$

where s is the square of the center-of-mass energy and J is the corresponding Jacobian. The multiplicity density $dN/d\eta$ in expression (13) concerns particular hadrons species. It depends on the center-of-mass energy, on various multiplicity selection criteria, and also on the production angles at which the inclusive spectra were measured. The procedure of obtaining the corresponding values of $dN/d\eta$ from the p_T spectra is described in [5]. The function $\psi(z)$ is normalized as follows:

$$\int_0^{\infty} \psi(z) dz = 1. \quad (14)$$

The above relation allows us to interpret the function $\psi(z)$ as a probability density to produce an inclusive particle with the corresponding value of the variable z .

2. SELF-SIMILARITY OF PION PRODUCTION IN pp COLLISIONS

Let us remind the main features of the z -scaling in proton–proton interactions characterized by a proton fractal dimension $\delta_1 = \delta_2 \equiv \delta$ in the initial state. Experimental data on inclusive cross sections of charged and identified hadrons measured in pp collisions at FNAL, ISR, and RHIC have been analyzed in [5,6]. The data cover a wide range of the collision energy, transverse momenta, and angles of the produced particles. Spectra from minimum-biased events and events with various multiplicity selection criteria have been studied in [7]. The energy, angular, and multiplicity independence of the scaling function $\psi(z)$ was established. It gives strong constraints on the values of the parameters c , δ , and ϵ . It was shown that the parameters are constant in a large kinematical region. None of the parameters depends on multiplicity. The scaling is consistent with $c = 0.25$ and $\delta = 0.5$ for all types of the analyzed inclusive hadrons. The value of ϵ increases with hadron mass [6].

Some results of the analysis are illustrated on the experimental data [9–12] depicted by different symbols in Fig.2, *a*. The data cover large range of the collision energies $\sqrt{s} = 19$ –200 GeV and transverse momenta $p_T = 0.2$ –10 GeV/ c of the produced hadrons. The distributions were measured in the central interaction region at $\theta_{\text{cms}} = 90^\circ$. The scaling function $\psi(z)$ is shown in Fig.2, *b* where the charged hadron spectra at different energies are «collapsed» onto a single curve. The behavior of $\psi(z)$ is described by the power law, $\psi(z) \sim z^{-\beta}$, in the asymptotic high- z (high- p_T) region.

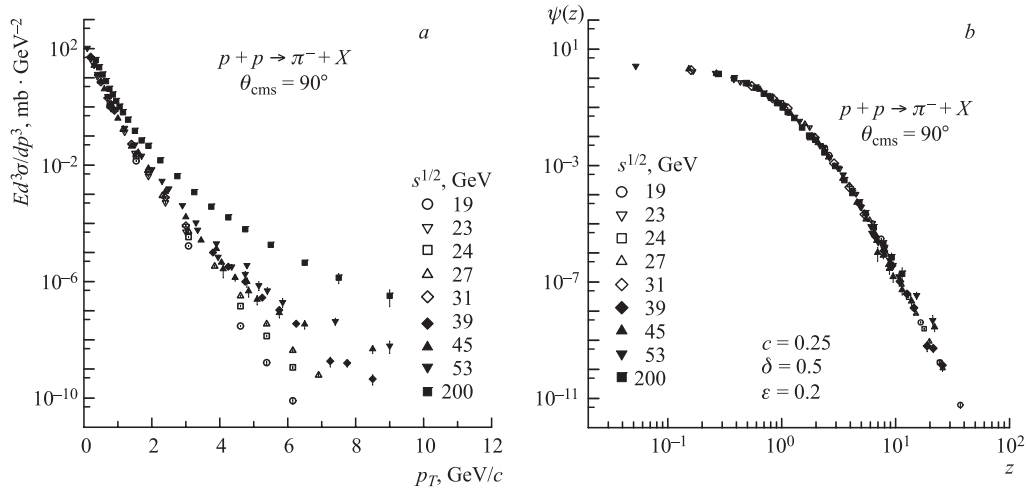


Fig. 2. *a*) Transverse momentum spectra of the π^- mesons produced in pp collisions at $\sqrt{s} = 19$ –200 GeV. Experimental data are taken from [9–12]. *b*) The corresponding scaling function $\psi(z)$

3. SELF-SIMILARITY OF PION PRODUCTION IN AA COLLISIONS

Here we present some ideas how to quantify energy losses of the produced particles, exploiting a specific connection between the suppression of the inclusive spectra in nuclear collisions and the corresponding multiplicity densities in dependence on the collision centrality. The ideas are motivated by the assumption of self-similarity of hadron interactions at a

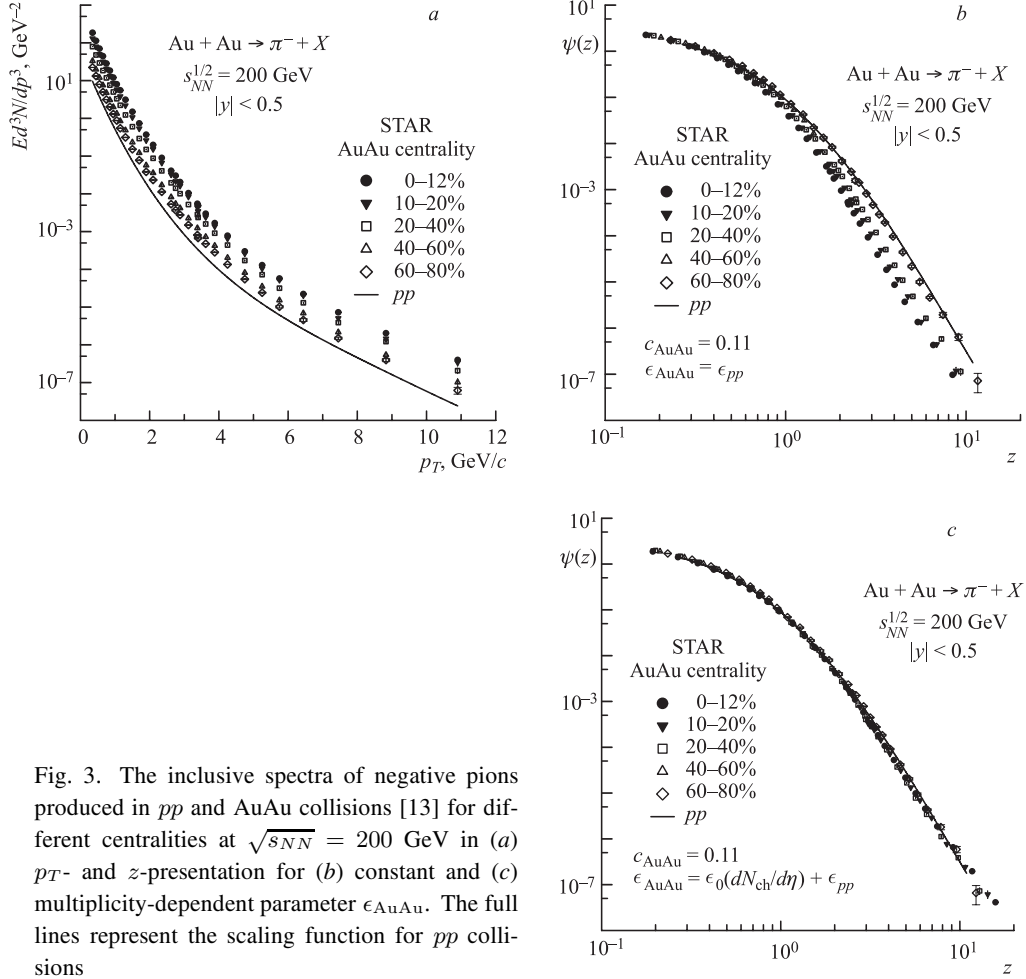


Fig. 3. The inclusive spectra of negative pions produced in pp and AuAu collisions [13] for different centralities at $\sqrt{s_{NN}} = 200$ GeV in (a) p_T - and z -presentation for (b) constant and (c) multiplicity-dependent parameter ϵ_{AuAu} . The full lines represent the scaling function for pp collisions

constituent level in both pp and AA collisions. This is demonstrated on pion spectra obtained at RHIC and SpS.

The STAR collaboration measured the spectra of negative pions [13] produced in AuAu collisions at $\sqrt{s_{NN}} = 200$ GeV. The spectra were taken at various centralities characterized by different multiplicity densities $dN_{ch}/d\eta|_0$ of charged particles produced in the central interaction region.

They cover a wide range of the transverse momentum, $p_T = 0.35-10.86$ GeV/c. The yields (Fig. 3, a) change more than eight orders of magnitude in this range. The centrality dependence of the pion spectra is plotted in z -presentation in Fig. 3, b. The corresponding pp data are represented by the full line. The parameter $\epsilon \equiv \epsilon_\pi = 0.2$ was fixed at the same value as for scaling analysis of pions in the pp collisions. The fractal dimension δ_{Au} of the colliding nuclei was determined in accordance with the additive property $\delta_A = A\delta$ obtained for pA interactions [14] with the same value of $\delta = 0.5$ as for pp data. The corresponding total multiplicity densities $dN_{ch}/d\eta|_0$ of charged particles produced in AuAu collisions have

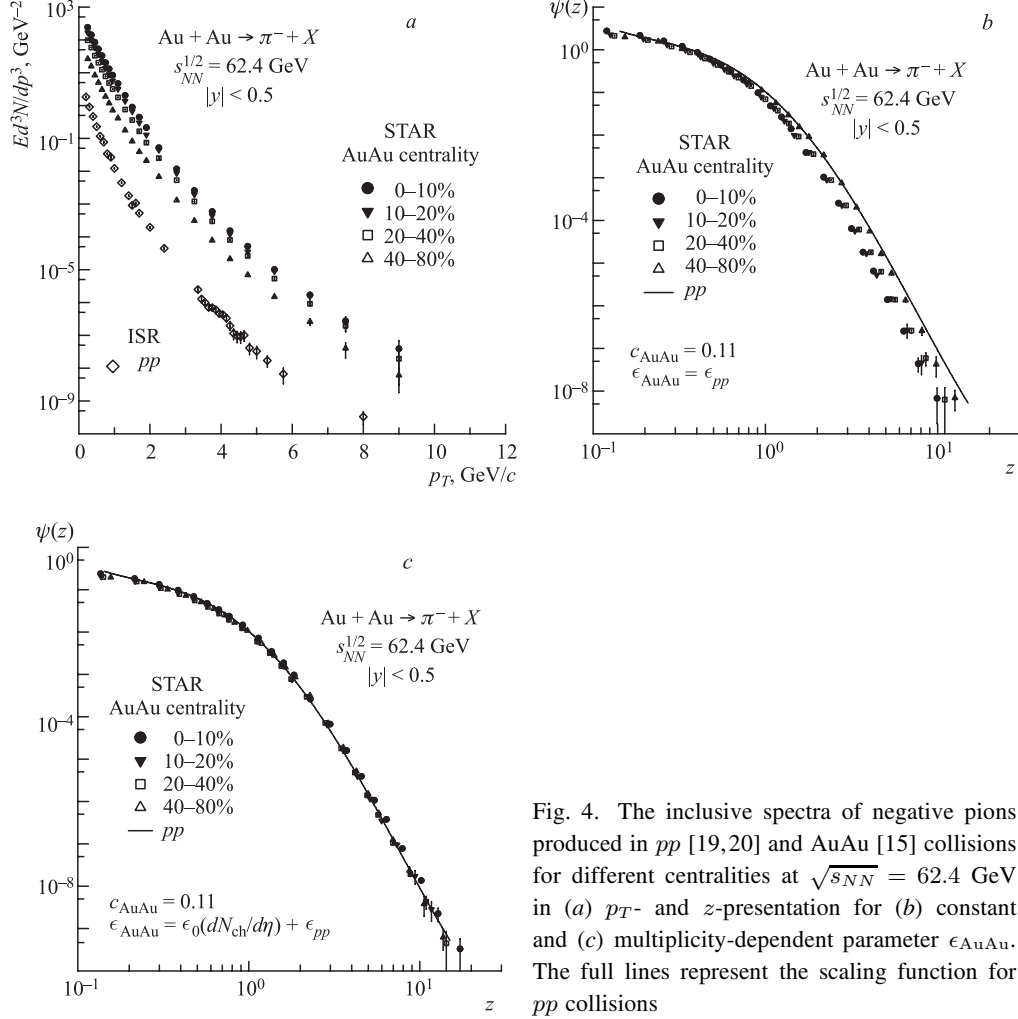


Fig. 4. The inclusive spectra of negative pions produced in pp [19,20] and AuAu [15] collisions for different centralities at $\sqrt{s_{NN}} = 62.4$ GeV in (a) p_T - and z -presentation for (b) constant and (c) multiplicity-dependent parameter ϵ_{AuAu} . The full lines represent the scaling function for pp collisions

been used in formula (9). They depend on the centrality of the nuclear collisions. In the case of pp interactions, the multiplicity density $dN_{ch}/d\eta|_0$ for the non-single-diffractive pp events was used in (9) for comparative reasons.

As seen from Fig. 3, *b*, the spectra in pp and peripheral AuAu collisions coincide with each other with good accuracy in z -presentation for $c_{AuAu} = 0.11$. This value is consistent with the energy independence of z -presentation of the pion spectra in the peripheral AuAu collisions. The result indicates that the form of the pion spectra in peripheral collisions is insensitive to modifications of the production mechanism by nuclear medium when compared with pp interactions. The influence of nuclei is included here with a drop-off in the «specific heat» c from its value $c_{pp} = 0.25$ obtained in pp collisions. One can see from Fig. 3, *b* that the AuAu spectra are suppressed in the high- z region relative to the pp scaling function $\psi(z)$ as the centrality increases. The largest suppression is for the most central collisions.

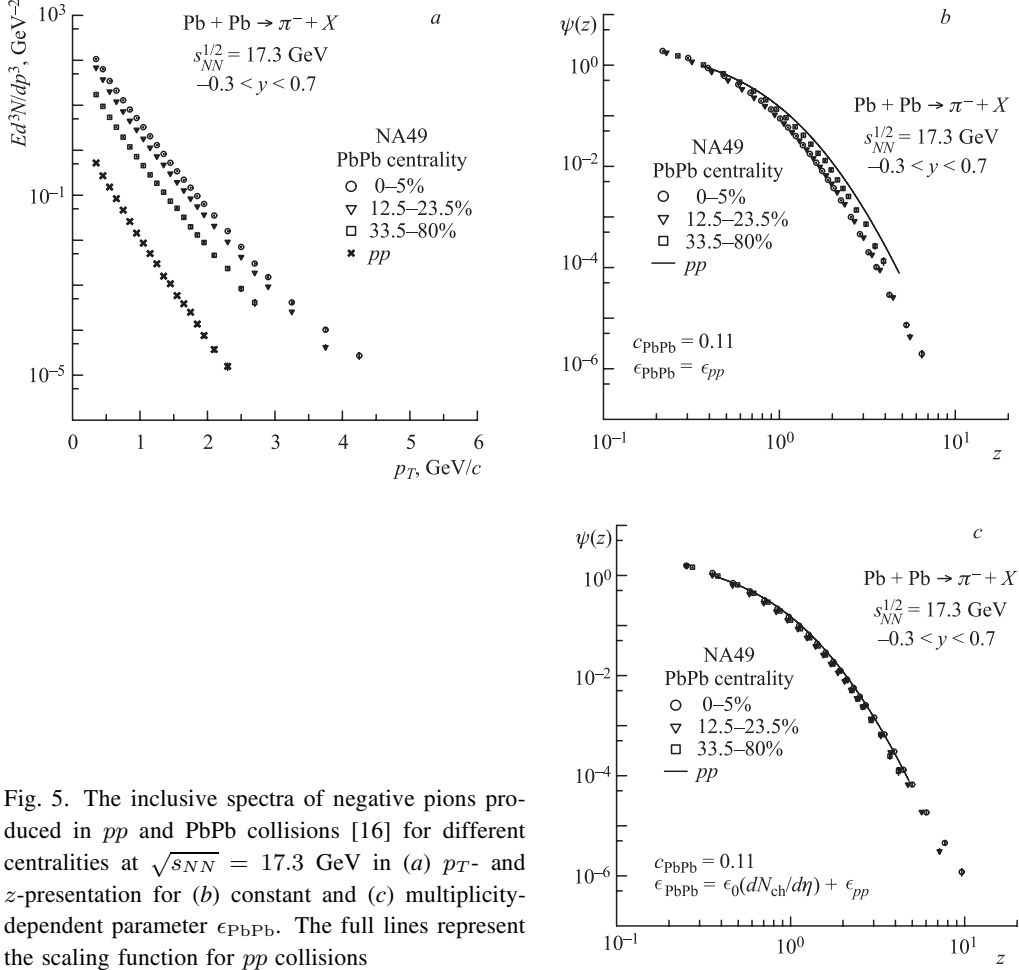


Fig. 5. The inclusive spectra of negative pions produced in pp and PbPb collisions [16] for different centralities at $\sqrt{s_{NN}} = 17.3$ GeV in (a) p_T - and z -presentation for (b) constant and (c) multiplicity-dependent parameter ϵ_{PbPb} . The full lines represent the scaling function for pp collisions

The same scaling behavior as for pp collisions can be obtained for AuAu interactions for all centralities. As shown in Fig. 3, c, this can be achieved by the parameter ϵ_{AA} allowing it to be a function of the multiplicity density $dN_{ch}/d\eta$. For that purpose we have used the parametrization

$$\epsilon_{AA} = \epsilon_0 \left(\frac{dN_{ch}}{d\eta} \right) + \epsilon_{pp} \quad (15)$$

with a suitable choice of the coefficient ϵ_0 . For AuAu collisions at $\sqrt{s_{NN}} = 200$ GeV we obtained $\epsilon_0 = 0.0028$. The increase of ϵ with the multiplicity density is connected with a decrease of the momentum fractions y_a and y_b . This results in larger energy losses in the final state. The energy losses depend on the amount of the traversed medium which converts them into the multiplicity of the produced particles. The larger ϵ the more energy losses of the secondary particles. The multiplicity density characterizes the produced medium and is connected in a such way to the energy losses in this medium.

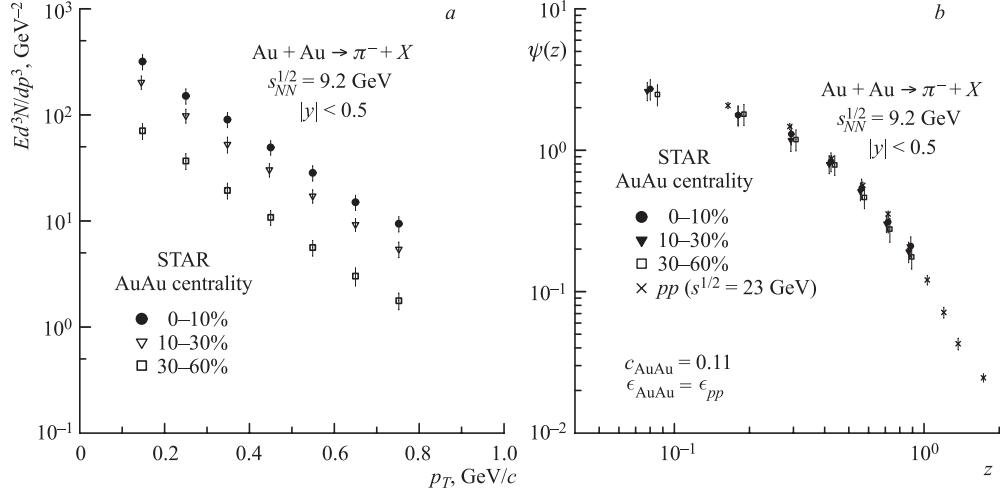


Fig. 6. The inclusive spectra of negative pions produced in AuAu collisions [17] for different centralities at $\sqrt{s_{NN}} = 9.2$ GeV in (a) p_T - and (b) z -presentation for constant parameter ϵ_{AuAu}

Results of similar analysis of the STAR data [15] on pion spectra at different centralities in AuAu collisions at $\sqrt{s_{NN}} = 62.4$ GeV are shown in Fig. 4. We have obtained $\epsilon_0 = 0.0018$ in this case.

The NA49 collaboration measured the transverse momentum spectra of negative pions [16] in PbPb collisions at $\sqrt{s_{NN}} = 17.3$ GeV. The invariant yields were extracted as a function of the transverse momentum p_T in the range from 0.3 to 4.5 GeV/c in the rapidity interval $-0.3 < y < 0.7$ at different collision centralities. Figure 5 demonstrates data on pion spectra with three centrality ranges in p_T - (plot a) and z -presentation without (plot b) and with (plot c) centrality dependence of ϵ_{PbPb} . As seen from Fig. 5, b, the shape of the function $\psi(z)$ at $\epsilon_{PbPb} = \epsilon_{pp}$ depends on centrality. The uniform shape can be restored with $\epsilon_0 = 0.0010$ (15) and $c_{PbPb} = 0.11$. The solid line shown in Fig. 5, c corresponds to pp data at the same energy.

The STAR collaboration measured for the first time the identified particle spectra in AuAu collisions at $\sqrt{s_{NN}} = 9.2$ GeV [17]. The restricted data sample (3000 events) allows one to compare the hadron yields, particle ratios or $\langle p_T \rangle$ to the same quantities obtained from SpS experiments at similar beam energies. The transverse momentum distributions at different centralities cover the range $p_T = 0.15-0.75$ GeV/c and $|\eta| < 0.5$.

The spectra of π^- mesons in p_T - and z -presentations are shown in Fig. 6, a and b, respectively. As seen from Fig. 6, b, the experimental data points do not reveal any dependence of ϵ_{AuAu} on centrality in this p_T range. Sensitivity of the shape of $\psi(z)$ to the collision centrality is expected to be enhanced for $z > 1$. A verification of the power law, $\psi(z) \sim z^{-\beta}$, of the scaling function for $z > 4$ is of interest in this energy region as well. A self-similarity of hadron substructure, constituent interactions, and fragmentation processes is visible in the pion spectra at higher energies. Measurements of pion distributions at $\sqrt{s_{NN}} = 9.2$ GeV in the range $p_T = 2-3$ GeV/c is therefore desirable to study centrality dependence of the energy losses in this energy region.

4. SELF-SIMILARITY OF PION PRODUCTION IN dAu COLLISIONS

We have analyzed data [18] on the transverse momentum distributions of pion spectra in dAu collisions at $\sqrt{s_{NN}} = 200$ GeV and $|\eta| < 0.5$. The pion yields measured over a range of $p_T = 0.2-9.5$ GeV/ c at different centralities are shown in p_T - and z -presentations in Fig. 7.

The fractal dimensions for deuteron and gold are $\delta_d = 2\delta$ and $\delta_{Au} = 197\delta$, respectively. The «specific heat» of the produced matter in this process is found to be $c = 0.23$, which is nearly the same as in proton–proton collisions ($c_{pp} = 0.25$). This value does not depend on kinematical parameters. Figure 7, c shows that centrality independence of the shape of the function $\psi(z)$ can be restored (the same shape for pp and dAu) if the fractal dimension ϵ_{dAu} of the fragmentation processes is assumed to be in the form (15). An indication of the power behavior of $\psi(z)$ is seen at high z . The values of the parameter ϵ_0 depend on the system size and collision energy. We have obtained $\epsilon_0(dAu) = 0.04 > \epsilon_0(CuCu) = 0.008 > \epsilon_0(AuAu) = 0.0028$ at $\sqrt{s_{NN}} = 200$ GeV. In this sense, the parameter ϵ_0 does not represent

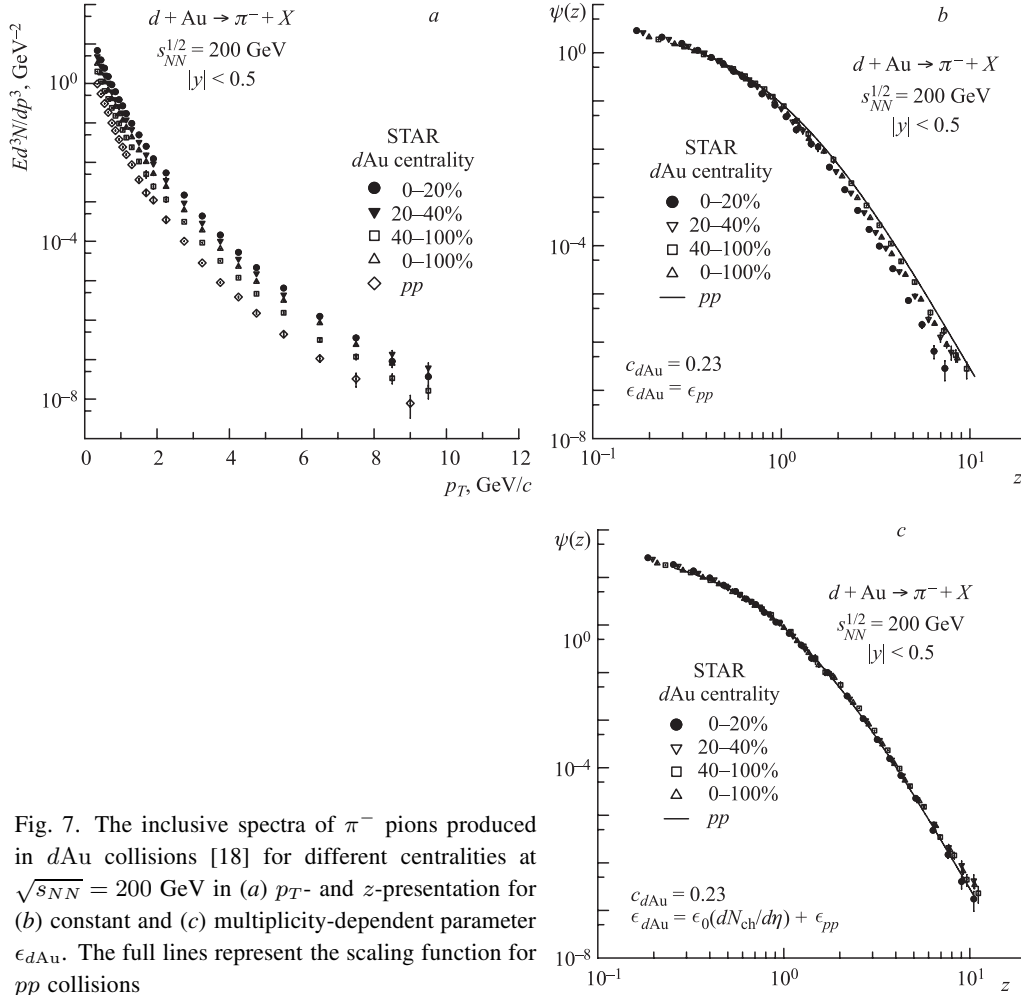


Fig. 7. The inclusive spectra of π^- pions produced in dAu collisions [18] for different centralities at $\sqrt{s_{NN}} = 200$ GeV in (a) p_T - and z -presentation for (b) constant and (c) multiplicity-dependent parameter ϵ_{dAu} . The full lines represent the scaling function for pp collisions

a scaling universal quantity. Its energy and system size dependence characterizes different energy losses discussed in the next section.

5. ENERGY LOSSES IN TERMS OF MOMENTUM FRACTIONS

In this section we use a microscopic scenario of particle production in terms of momentum fractions for estimation of the energy losses of the produced particles in nuclear medium. In the framework of such a scenario, any inclusive particle is characterized by the quantity z . It consists of the finite part z_0 and of the divergent factor Ω^{-1} . The factor Ω^{-1} depends on the momentum fractions x_1, x_2 and y_a, y_b which carry the incoming constituents and the inclusive particle (m_1) with its counterpart (m_2), respectively. The variable z is the scale-dependent quantity. The principle of minimal resolution Ω^{-1} allows us to fix the values of the momentum fractions x_1, x_2, y_a , and y_b and single out the most effective binary subprocess which underlies the inclusive reaction. The recoil mass M_X characterizes dissipation of the recoil object moving in the away side of the inclusive particle. The quantities y_a and M_X are therefore important ingredients of the fragmentation process. Some dependences of the momentum fraction x_1, x_2, y_a, y_b and the recoil mass M_X on the transverse momentum p_T of π^- mesons produced in pp , AuAu, and PbPb collisions are shown in Figs. 8–12.

5.1. Momentum Fractions versus p_T . Study of the momentum fractions and their dependences on the collision energy, centrality, and transverse momentum of the inclusive particle gives us possibility to look at the microscopic picture of the underlying subprocesses. The fractions x_1 and x_2 characterize amount of the energy (momentum) of the interacting nuclei carried by their constituents which undergo the binary collision (2). The fractions y_a and y_b characterize energy losses of the scattered and recoil constituents during their fragmentation in vacuum for pp collisions or in medium in the case of nuclear interactions.

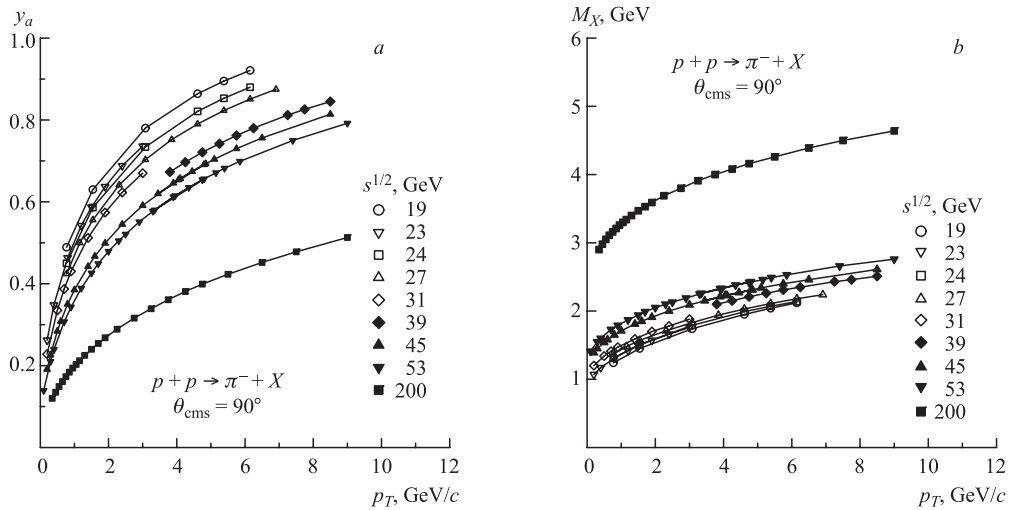


Fig. 8. The dependence of the fractions y_a (a) and the recoil mass M_X (b) on the transverse momentum p_T for π^- mesons produced in pp collisions at $\theta_{\text{cms}} = 90^\circ$ and different collision energies

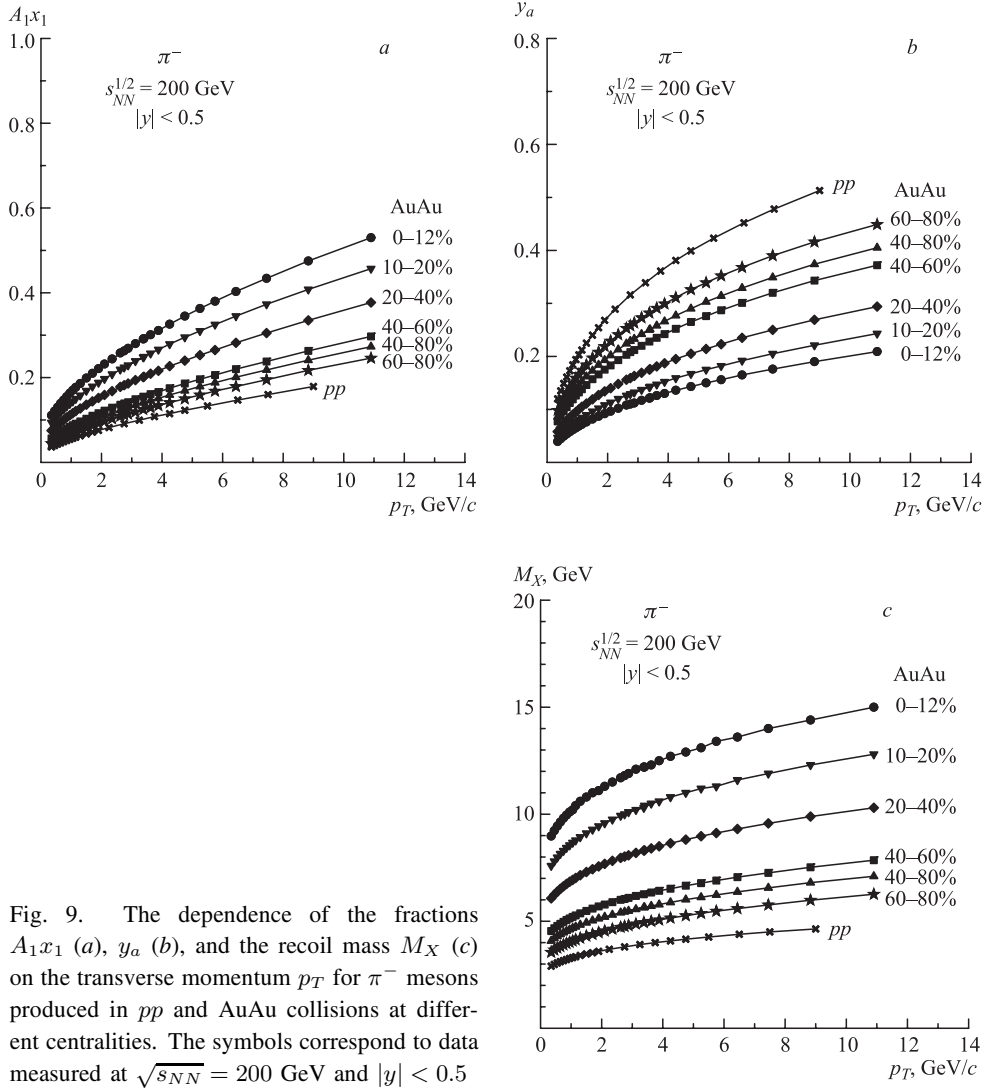


Fig. 9. The dependence of the fractions A_1x_1 (a), y_a (b), and the recoil mass M_X (c) on the transverse momentum p_T for π^- mesons produced in pp and AuAu collisions at different centralities. The symbols correspond to data measured at $\sqrt{s_{NN}} = 200$ GeV and $|y| < 0.5$

Figure 8 shows the dependence of the fraction y_a (plot a) and the recoil mass M_X (plot b) on the transverse momentum of pions produced in pp collisions at $\sqrt{s} = 19\text{--}200$ GeV and $\theta_{\text{cms}} = 90^\circ$. As seen from Fig. 8, a, the energy loss characterized by a deviation of the fraction y_a from unity decreases with the increasing momentum p_T and increases with the collision energy \sqrt{s} . Let us consider a pion with the momentum 6 GeV/c produced in pp collisions. In the presented scenario, the pion is produced by fragmentation of a secondary parton with the momentum $p_T = 6/0.9 = 6.6$ or $6/0.4 = 15$ GeV/c at $\sqrt{s} = 19$ or 200 GeV, respectively. This quantitative comparison characterizes increase of the energy losses with the collision energy. The recoil mass M_X increases with both the energy and pion transverse momentum in a way shown in Fig. 8, b.

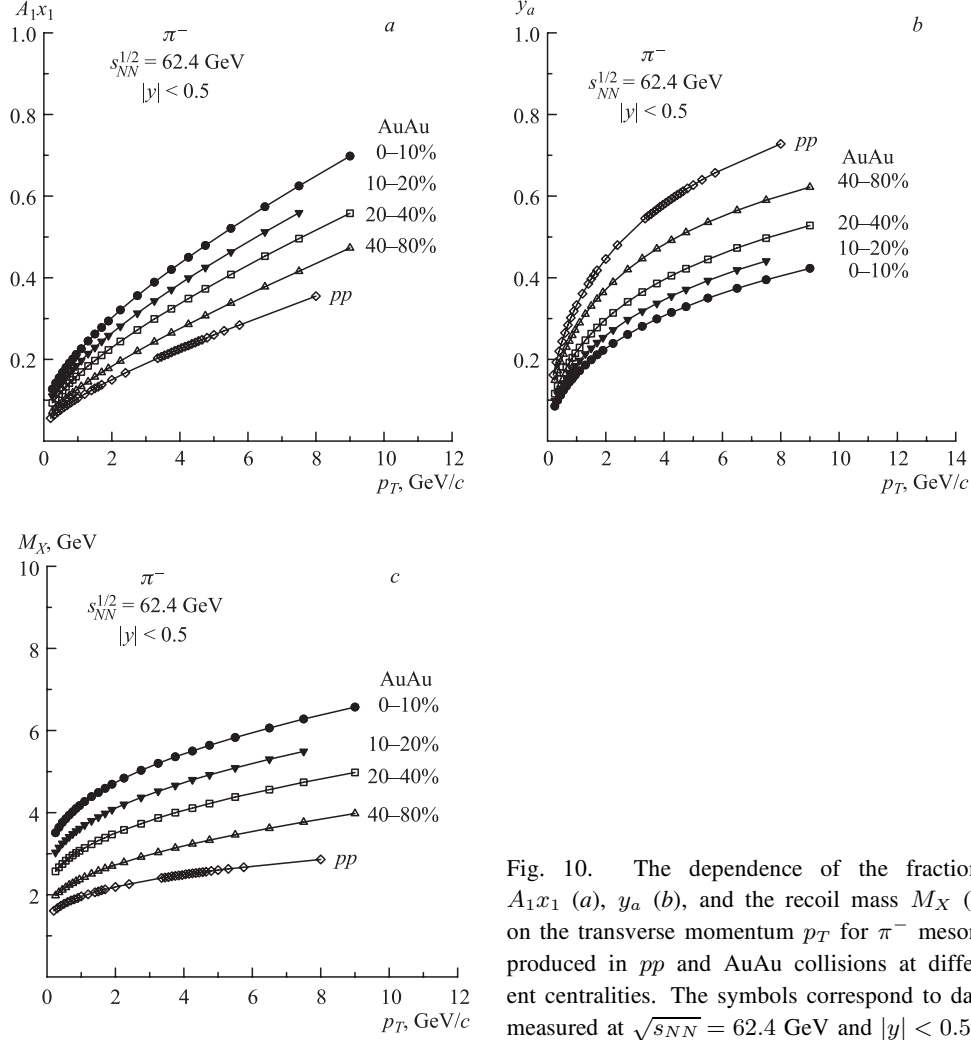


Fig. 10. The dependence of the fractions $A_1 x_1$ (a), y_a (b), and the recoil mass M_X (c) on the transverse momentum p_T for π^- mesons produced in pp and AuAu collisions at different centralities. The symbols correspond to data measured at $\sqrt{s_{NN}} = 62.4$ GeV and $|y| < 0.5$.

Figures 9, a, 10, a, 11, a, and 12, a demonstrate the dependence of the momentum fraction x_1 expressed in units of nucleon mass on the transverse momentum p_T of negative pions produced in AA collisions at $\sqrt{s_{NN}} = 200, 62.4, 17.3,$ and 9.2 GeV, respectively. The points correspond to data at $\theta_{\text{cms}} \simeq 90^\circ$. Both fractions x_1 and x_2 are equal to each other in this case. The fraction x_1 increases with the transverse momentum p_T and centrality. For fixed p_T , x_1 decreases as the collision energy \sqrt{s} increases.

Figures 9, b, 10, b, 11, b, and 12, b show the dependences of the momentum fractions y_a on the kinematical (p_T, \sqrt{s}) and dynamical ($dN_{\text{ch}}/d\eta$) variables. They describe features of the fragmentation process. The fraction y_a characterizes dissipation (energy loss) of the momentum of the object produced in the underlying constituent interaction into the near side of the inclusive particle. The behavior of y_a demonstrates a monotonic growth with p_T . It means that the energy losses associated with the production of a high- p_T pion are smaller

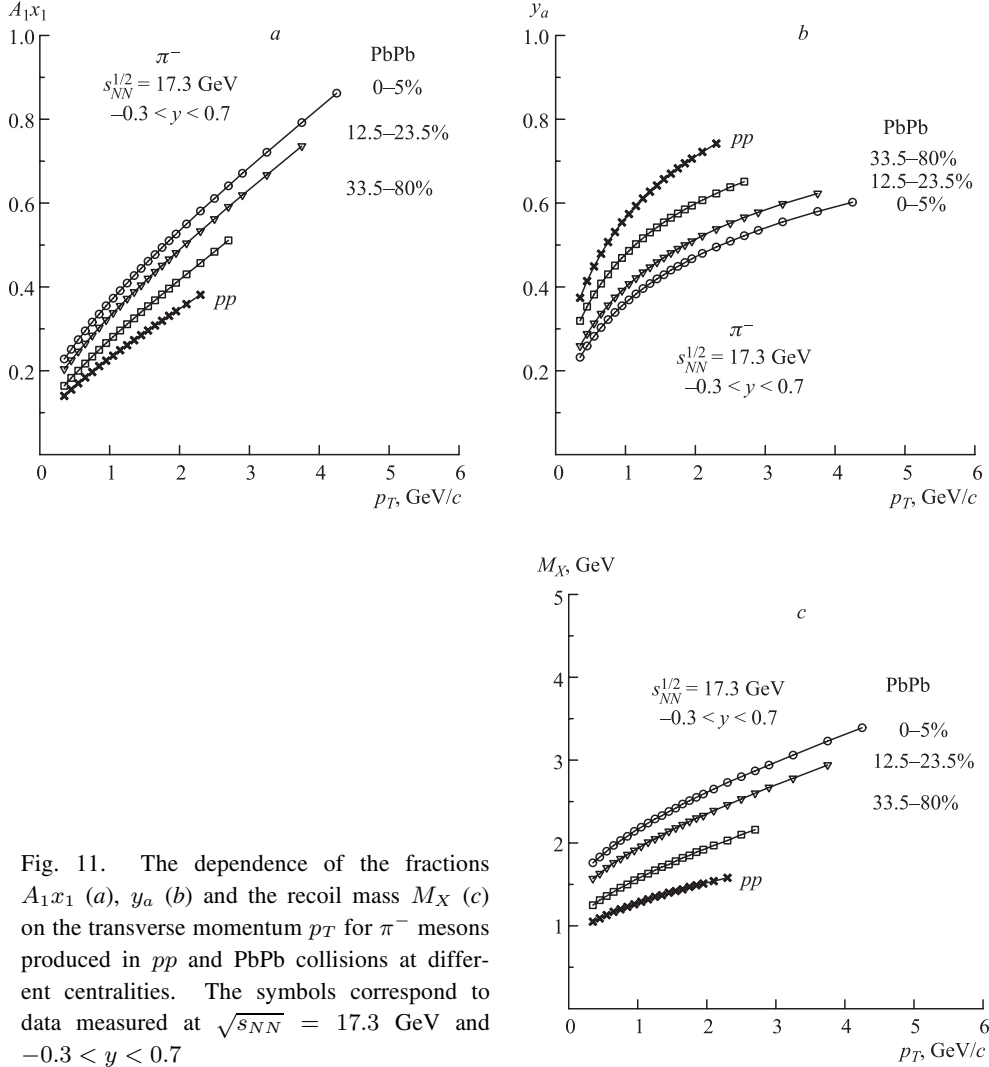


Fig. 11. The dependence of the fractions $A_1 x_1$ (a), y_a (b) and the recoil mass M_X (c) on the transverse momentum p_T for π^- mesons produced in pp and PbPb collisions at different centralities. The symbols correspond to data measured at $\sqrt{s_{NN}} = 17.3$ GeV and $-0.3 < y < 0.7$

than for the inclusive processes with lower transverse momenta. The decrease of y_a with centrality in AuAu and PbPb collisions represents larger energy losses in the central collisions as compared with the pp and peripheral AA interactions. Energy dissipation grows as the collision energy increases. Let us consider for definiteness a pion produced in the central AuAu collisions (0-12%) at $\sqrt{s_{NN}} = 200$ GeV which has the momentum $p_T = 4$ GeV. The pion was formed in the fragmentation of the secondary parton produced in the constituent interaction with the momentum $p_T = 4/0.1 = 40$ GeV. The momenta of such partons decrease with the decreasing collision energy and are equal to $4/0.3 = 13$ and $4/0.55 = 7.3$ GeV/c at $\sqrt{s_{NN}} = 62.4$ and 17.3 GeV, respectively. The fraction y_a follows the general trend, i.e., a decrease with the collision energy and centrality, and a growth with the transverse momentum p_T .

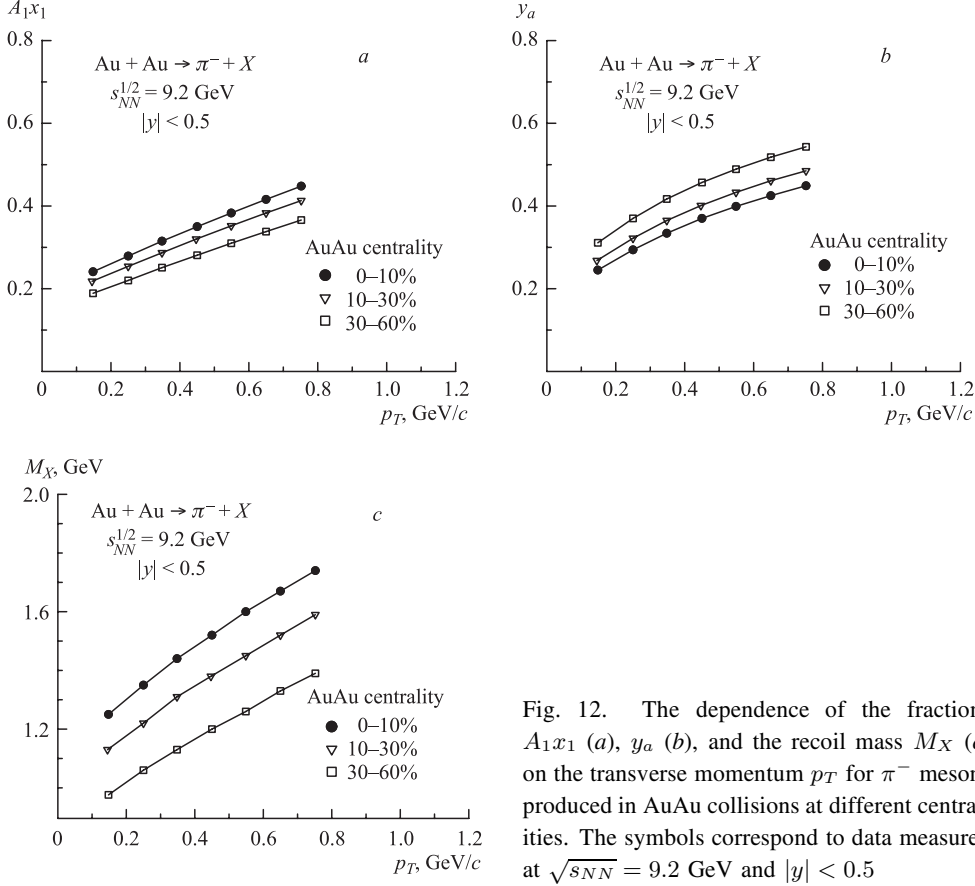


Fig. 12. The dependence of the fractions $A_1 x_1$ (a), y_a (b), and the recoil mass M_X (c) on the transverse momentum p_T for π^- mesons produced in AuAu collisions at different centralities. The symbols correspond to data measured at $\sqrt{s_{NN}} = 9.2$ GeV and $|y| < 0.5$

The fraction y_b governs the recoil mass M_X characterizing the dissipation of the energy and momentum in the away side direction of the inclusive particle. It was found that y_b is much smaller than y_a at high p_T . The small values of y_b mean that the momentum of the inclusive particle is more likely balanced by a multiple system consisting of many low-momentum particles moving in the opposite direction. The fraction y_b decreases with the increasing collision energy \sqrt{s} . Its dependence on p_T and centrality is weak. Both fractions become equal to each other, $y_a \simeq y_b$, at low transverse momenta. The equality at low p_T remains preserved independent of \sqrt{s} .

5.2. Mass of Recoil System versus p_T . The recoil mass M_X of the system associated with production of the inclusive particle is defined by the expression

$$M_X = x_1 M_1 + x_2 M_2 + \frac{m_2}{y_b}. \quad (16)$$

The quantity is proportional to the momentum fractions x_1 and x_2 of the interacting objects with the masses M_1 and M_2 . It has connection with the fractions y_a and y_b via the dependences $x_{1,2} = x_{1,2}(y_a, y_b)$ (see [5]) which include the fractal dimensions δ_1 and δ_2 . The correlation between these quantities is reflected in symmetry properties of the function $\psi(z)$.

The recoil mass M_X reflects therefore an internal connection to the structure of the colliding objects, constituent interactions, and process of formation of the individual hadrons.

Figures 9, *c*, 10, *c*, 11, *c*, and 12, *c* show the dependence of the recoil mass on the transverse momenta of the negative pions produced in the central rapidity region in AuAu and PbPb collisions at the energy $\sqrt{s_{NN}} = 200, 62.4, 17.3,$ and 9.2 GeV. All the curves demonstrate growth with p_T which is followed at $\sqrt{s_{NN}} = 62.4$ and 200 GeV by a successive flattening. The dependences reveal a characteristic increase with the collision energy. The growth of M_X with p_T is larger for nucleus collisions in comparison with its slight increase for pp interactions. The values of M_X and their growth with p_T become larger with the collision centrality. This means that the momentum balance in a subprocess underlying the pion production is compensated with growing number of particles moving in the away side direction when the centrality of the nuclear collisions increases. Considering an example of an inclusive pion with the momentum $p_T = 4$ GeV/ c , the corresponding recoil masses M_X in the central AuAu and PbPb collisions are equal to 3.5, 5.5, and 13 GeV at the energy $\sqrt{s_{NN}} = 17.3, 62.4,$ and 200 GeV, respectively.

5.3. Scale Dependence of Energy Losses.

The developed microscopic scenario of hadron production in nucleus–nucleus collisions allow us to study the scale dependence of the energy losses. We would like to remind that the variable z is scale-dependent quantity. It has properties of a fractal measure depending on the fractal dimensions δ and ϵ . The energy losses by the creation of the inclusive particle are described in terms of the momentum fraction y_a . The dependence of y_a on z characterizes the energy losses at different scales. We assume that those scales where the energy losses are largest are most preferable for searching for a phase transition of nuclear matter.

Figure 13 shows the scale dependence of y_a (connected with energy loss) for central AA collisions at $\sqrt{s_{NN}} = 200, 62.4, 17.3,$ and 9.2 GeV. The energy loss decreases as the resolution with respect to the constituent subprocesses increases. At high z , a saturation of the scale density of energy loss (dy_a/dz) for all energies is expected.

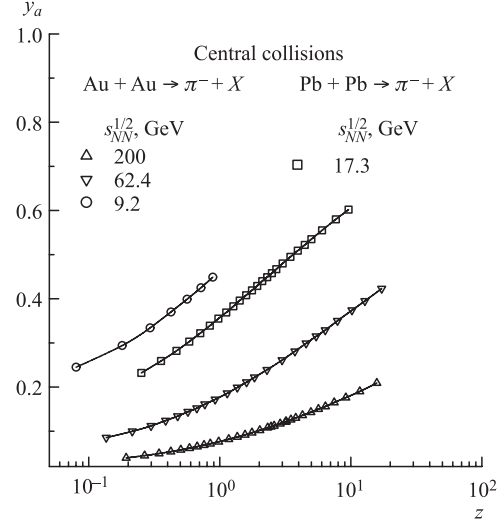


Fig. 13. The dependence of y_a on z for π^- mesons produced in central AuAu and PbPb collisions at $\sqrt{s_{NN}} = 200, 62.4, 17.3,$ and 9.2 GeV

CONCLUSIONS

Experimental data on inclusive spectra of negative pions produced in AuAu collisions at RHIC energies $\sqrt{s_{NN}} = 200, 62.4,$ and 9.2 GeV were analyzed in the framework of z -scaling. The results are compared with the NA49 data on pion spectra measured in pp and PbPb collisions at $\sqrt{s_{NN}} = 17.3$ GeV. The experimental data in z -presentation indicate similarity

as a characteristic feature of mechanism of pion production. It was argued that this property includes structure of the colliding objects, interaction of their constituents, and character of the fragmentation process. A microscopic scenario of nucleus–nucleus interactions at a constituent level in terms of momentum fractions was developed. The z -presentation of the pion spectra in AuAu and PbPb collisions reveal scaling features identical with the z -scaling in the elementary collisions.

The parameter c interpreted as «specific heat» of the medium produced in heavy-ion collisions was established to decrease with the increasing system size, $c_{pp} = 0.25 > c_{dAu} = 0.23 > c_{CuCu} = 0.14 > c_{AuAu} = 0.11$. The values of c are independent of the collision energy and centrality. The fractal dimension dependence $\epsilon_{AA} = \epsilon_0(dN_{ch}/d\eta) + \epsilon_{pp}$ of the fragmentation process on collision centrality allows us to restore the unique shape of the scaling function for pp and AA collisions over a wide range of z . In the hard p_T region (large z), the scaling function manifests typical power behavior, $\psi(z) \simeq z^{-\beta}$, with a constant value of the slope parameter β . We have estimated the energy losses of the secondary partons passing through the medium created in the nuclear collisions. They depend on the collision energy, transverse momentum, and centrality. It was shown that energy loss increases in a specific manner with the collision energy and centrality, and decreases with p_T . The scale dependence of energy losses was studied. The obtained results may be exploited to search for and study new physics phenomena in pion production in heavy-ion collisions at U70, RHIC, LHC, and at the proposed projects NICA and FAIR.

The investigations have been supported by the IRP AVOZ10480505, by the Grant Agency of the Czech Republic under Contract No.202/07/0079, and by the special program of the Ministry of Science and Education of the Russian Federation, grant RNP.2.1.1.2512.

REFERENCES

1. Adams J. et al. (STAR Collab.) // Phys. Rev. Lett. 2003. V. 91. P. 172302.
2. Arsene I. et al. (BRAHMS Collab.) // Ibid. P. 172305.
3. Adler S. S. et al. (PHENIX Collab.) // Phys. Rev. C. 2004. V. 69 P. 034910.
4. Back B. B. et al. (PHOBOS Collab.) // Phys. Rev. Lett. 2005. V. 94. P. 082304.
5. Zborovský I., Tokarev M. V. // Phys. Rev. D. 2007. V. 75. P. 094008.
6. Zborovský I., Tokarev M. V. // Intern. J. Mod. Phys. A. 2009. V. 24. P. 1.
7. Tokarev M. V., Zborovský I. // Phys. At. Nucl. 2007. V. 70. P. 1294.
8. Stavinsky V. S. // Sov. J. Part. Nucl. 1979. V. 10. P. 949.
9. Antreasyan D. et al. // Phys. Rev. D. 1979. V. 19. P. 764.
10. Alper B. et al. (BS Collab.) // Nucl. Phys. B. 1975. V. 100. P. 237.
11. Jaffe D. E. et al. // Phys. Rev. D. 1989. V. 40. P. 2777.
12. Adams J. et al. (STAR Collab.) // Phys. Lett. B. 2006. V. 637. P. 161.

13. *Abelev B. I. et al. (STAR Collab.) // Phys. Rev. Lett.* 2006. V. 97. P. 152301.
14. *Zborovský I. et al. // Phys. Rev. C.* 1999. V. 59. P. 2227.
15. *Abelev B. I. et al. (STAR Collab.) // Phys. Lett. B.* 2007. V. 655. P. 104.
16. *Alt C. et al. (NA49 Collab.) // Phys. Rev. C.* 2008. V. 77. P. 034906.
17. *Kumar L. et al. (STAR Collab.) // Proc. of «Strange Quark Matter 2008», Beijing, China, Oct. 6–10, 2008; <http://qm.phys.tsinghua.edu.cn/thu-henp/2008/sqm2008/>; nucl-ex/0812.4099.*
18. *Adams J. et al. (STAR Collab.) // Phys. Lett. B.* 2006. V. 637. P. 161.
19. *Alper B. et al. (BS Collab.) // Nucl. Phys. B.* 1975. V. 100. P. 237.
20. *Büsser F. W. et al. (CCRS Collab.) // Nucl. Phys. B.* 1976. V. 106. P. 1.

Received on July 27, 2009.